

Published in final edited form as:

J Proteome Res. 2010 February 5; 9(2): 1104–1120. doi:10.1021/pr901076y.

Global analysis of TDP-43 interacting proteins reveals strong association with RNA splicing and translation machinery

Brian D. Freibaum¹, Raghu Chitta², Anthony A. High², and J. Paul Taylor^{1,*}

¹Department of Developmental Neurobiology, St. Jude Children's Research Hospital, Memphis, Tennessee 38105-3678, USA

²Hartwell Center for Bioinformatics and Biotechnology, St. Jude Children's Research Hospital, Memphis, Tennessee 38105-3678, USA

Abstract

TDP-43 is a highly conserved and ubiquitously expressed member of the heterogeneous nuclear ribonucleoprotein (hnRNP) family of proteins. Recently, TDP-43 was shown to be a major disease protein in the ubiquitinated inclusions characteristic of most cases of amyotrophic lateral sclerosis (ALS), *tau*-negative frontotemporal lobar degeneration (FTLD), and inclusion body myopathy. In these diseases, TDP-43 is redistributed from its predominantly nuclear location to ubiquitin-positive, cytoplasmic foci. The extent to which TDP-43 drives pathophysiology is unknown, but the identification of mutations in TDP-43 in familial forms of ALS and FTLD-U suggests an important role for this protein in pathogenesis. Little is known about TDP-43 function and only a few TDP-43 interacting proteins have been previously identified, which makes further insight into both the normal and pathological functions of TDP-43 difficult. Here we show, via a global proteomic approach, that TDP-43 has extensive interaction with proteins that regulate RNA metabolism. Some interactions with TDP-43 were found to be dependent on RNA-binding, whereas other interactions are RNA-independent. Disease-causing mutations in TDP-43 (A315T and M337V) do not alter its interaction profile. TDP-43 interacting proteins largely cluster into two distinct interaction networks, a nuclear/splicing cluster and a cytoplasmic/translation cluster, strongly suggesting that TDP-43 has multiple roles in RNA metabolism and functions in both the nucleus and the cytoplasm. Finally, we found numerous TDP-43 interactors that are known components of stress granules and, indeed, we find that TDP-43 is also recruited to stress granules.

Introduction

The RNA binding protein TDP-43¹ was recently identified as the major disease protein in the ubiquitinated inclusions characteristic of sporadic and familial forms of amyotrophic lateral sclerosis (ALS), *tau*-negative frontotemporal lobar degeneration (FTLD), and inclusion body myopathy. TDP-43 pathology also frequently accompanies the pathognomonic pathology of Parkinson's and Alzheimer's diseases²⁻⁴. In these diseases, TDP-43 is redistributed from its predominantly nuclear location to ubiquitin-positive, cytoplasmic foci. The extent to which TDP-43 drives pathophysiology is unknown, but the identification of mutations in TDP-43 underlying rare familial forms of ALS and FTLD suggests an important role for this protein in pathogenesis⁵⁻⁹.

*Corresponding author: J. Paul Taylor, MD, PhD, Associate Member, Department of Developmental Neurobiology, St. Jude Children's Research Hospital, MS 343, D-4026, 262 Danny Thomas Place, Memphis, TN 38105-3678, jpaul.taylor@stjude.org, Phone: (901) 595-6047, FAX: (901) 595-2032.

TDP-43 is a highly conserved and ubiquitously expressed member of the heterogeneous nuclear ribonucleoprotein (hnRNP) family of proteins¹⁰. TDP-43 contains two RNA recognition motifs (RRMs) and binds RNA primarily through the first of these¹. The glycine-rich C-terminus of TDP-43 has been shown to mediate interaction with several other hnRNP proteins, specifically hnRNPs A1, A2/B1, C1/C2, and A3¹¹, although the full extent of TDP-43 interactions has not been previously described. Predominantly a nuclear protein, TDP-43 has been shown to shuttle between the nucleus and cytoplasm¹². Interestingly, TDP-43 redistributes to cytosolic granules as a physiological response to neuronal injury, and nuclear localization is restored after recovery^{13, 14}.

Little is known about TDP-43 function, although there is evidence from experimental systems that TDP-43 can negatively regulate expression of target genes at multiple levels, including transcription, splicing and translation¹⁵⁻¹⁷, although the full extent of TDP-43 target genes and the influence of TDP-43 on their expression is not known. Additionally, there is no clear consensus of how pathological TDP-43 functions within diseased cells.

To date, only a few TDP-43 interacting proteins have been identified, which makes further insight into both the normal and pathological functions of TDP-43 difficult. Here we show, via a global proteomic approach, that TDP-43 has extensive interaction with proteins that regulate mRNA metabolism. TDP-43 interacting proteins largely cluster into two distinct protein interaction networks. The first is a network of nuclear proteins that regulate RNA splicing and other aspects of nuclear RNA metabolism, and the second is a network of cytoplasmic proteins that regulate mRNA translation. Additionally, we show that TDP-43 interaction with some proteins is dependent on TDP-43 interaction with RNA, whereas other interactions are RNA-independent. Surprisingly, the disease-causing mutations A315T and M337V do not alter the profile of TDP-43 interactions. Numerous proteins in translational regulation cluster are known to accumulate in stress granules and, indeed, we find that TDP-43 is also recruited to stress granules.

Methods

Plasmids

FLAG-TDP-43 was subcloned into the mammalian expression vector pcDNA 3.1(+)
(*Invitrogen*). FLAG-TDP-43(A315T), FLAG-TDP-43(M337V) and FLAG-TDP-43
(mutRRM) with the W113A and R151A mutations were generated using PCR to perform site-directed mutagenesis.

Immunoprecipitations/Immunoblot

10 cm² plates of HEK-293T or HeLa cells grown in a 1:1 mixture of DMEM/F12 culture media were transfected with 5µg of FLAG-TDP-43 or relevant TDP-43 mutant plasmid for 48 hours. Cells were then lysed in gentle lysis buffer (1X PBS, 5mM EDTA, 0.2% NP-40, 10% glycerol + Roche complete EDTA-free protease inhibitor cocktail Cat# 11836170001), passed five times through a 21-gauge needle, and spun at 20,000g for 10 minutes. The supernatant was pre-cleared using Protein G affinity gel (Sigma, Cat# E3403) for 30 minutes and then immunoprecipitated using Anti-FLAG M2 affinity gel (Sigma, Cat# F2426) for 1.5 hours at 4C. The immunoprecipitate was then eluted using FLAG peptide (Sigma, Cat# F3290) at 4C for 30 minutes. 330 µg of RNase A (Sigma, Cat# R4642) was added immediately following lysis prior to immunoprecipitation where indicated. For immunoprecipitation from mouse brain tissue, mouse brain homogenate was lysed as described above and then immunoprecipitated with 2.5 µg of TDP-43 polyclonal antibody (Proteintech, Cat# 10782-2-AP). As a control, half of the homogenate was immunoprecipitated using normal rabbit IgG.

Lysates/immunoprecipitates were separated on a 8-16% gradient tris-glycine gel. M2 monoclonal antibody (Sigma, Cat# F1804) and TDP-43 polyclonal antibody (Proteintech, Cat# 10782-2-AP) were used to visualize TDP-43. Polyclonal antibodies were also used to visualize PABPC1, hnRNP H and hnRNP U respectively (Abcam Cat# ab21060 and ab10374, Bethyl Laboratories Cat# A300-689A).

Immunofluorescence

HEK-293T cells grown on chamber slides (Lab-Tek Cat#154917) were transiently transfected with FLAG-TDP43 or FLAG-TDP-43(mutRRM) using FuGENE 6 (Roche Diagnostics). After 48 h, HEK-293T cells were fixed in 4% formaldehyde in PBS for 10 min at room temperature. The cells were then permeabilized with 0.5% Triton-X in PBS and incubated with primary antibodies for 1 hr to visualize TDP-43, hnRNP H, PABPC1, EIF4G and G3BP1. Cells were then washed and proteins were visualized using secondary antibodies conjugated to Rhodamine Red-X and FITC (Jackson ImmunoResearch). Cells were then washed, stained with DAPI and visualized on a Leica DMIRE2 fluorescent microscope using a 63X objective.

Antibodies

The following primary antibodies were used to visualize proteins: mouse anti-FLAG M2 (1:1000 for western blot and immunofluorescence) (Sigma Cat# F1804), rabbit anti-TDP-43 (1:350 for immunofluorescence) (Proteintech Group Cat# 10782-2-AP), rabbit anti-PABPC1 (1:1000 for western blot, 1:200 for immunofluorescence) (Abcam Cat# ab21060-100), rabbit anti-hnRNP H (1:10,000 western blot, 1:500 for immunofluorescence) (Abcam, Cat# 10374-50), mouse anti-G3BP1 (1:200 for immunofluorescence) (BD Transduction Laboratories Cat #611126), and rabbit anti-EIF4G (1:200 for immunofluorescence) (Santa Cruz Biotechnology Cat# sc-11373)

LC-MS/MS protein identification

FLAG epitope-tagged TDP-43 constructs were transfected into HEK293T cells and immunoprecipitated as described above. The sample was then run on an 8-16% gel, and analyzed as described below.

Enzymatic Digest of Proteins

The gel lane containing the immunoprecipitated sample was manually excised into 24 bands in the molecular weight range between 14 kDa and greater than 200 kDa. Each of the protein bands was then digested individually as below. The protein bands were cut into small plugs, washed with 50% acetonitrile, and destained by several incubations in 100 mM ammonium bicarbonate pH 8 containing 50% acetonitrile. Reduction (10 mM, DTT for 1 hour at 37°C) and alkylation (50 mM iodoacetamide for 45 min at room temperature in the dark) were performed, followed by washing of the gel plugs with 50% acetonitrile in 50mM ammonium bicarbonate twice. The gel plugs were then dried using a speedvac (Savant) and rehydrated in 10 µl of 0.2µg trypsin. 25uL of 25 mM ammonium bicarbonate pH 8 was added to the tube after 10 minutes. The peptides were extracted from the gel plugs using 20 to 30uL of 0.2% formic acid after an overnight (approx 12 hours) enzymatic reaction at 37°C. The solution was then transferred to a sample vial for LC-MS/MS analysis. Non-transfected cells were used as a control and treated in an identical manner to determine non-specific interactions.

Electrospray Ionization Ion Trap Mass Spectrometry Analysis

LC-MS/MS analysis was performed using a ThermoFisher LTQ XL linear ion trap mass spectrometer in line with a nanoAcquity ultra performance LC system (Waters Corporation, Milford, MA). Tryptic peptides generated above were loaded onto a "precolum" (Symmetry C18, 180µm i.d X 20mm, 5µm particle) (Waters Corporation, Milford, MA) which was

connected through a zero dead volume union to the analytical column (BEH C18, 75 μ m i.d X 100mm, 1.7 μ m particle) (Waters Corporation, Milford, MA). The peptides were then eluted over a gradient (0-70% B in 60 minutes, 70-100% B in 10 minutes, where B = 70% Acetonitrile, 0.2% formic acid) at a flow rate of 250nL/min and introduced online into the linear ion trap mass spectrometer (ThermoFisher Corporation, San Jose, CA) using electrospray ionization (ESI). Data dependent scanning was incorporated to select the 10 most abundant ions (one microscan per spectra; precursor isolation width 3.0Da, 35% collision energy, 30ms ion activation, exclusion duration: 30s; repeat duration: 15s; repeat count: 2) from a full-scan mass spectrum for fragmentation by collision activated dissociation (CAD).

Database Searching

Product ions generated above (b/y-type ions) were used in an automated database search against the Swissprot (Swissprot 57.1, *Homo Sapiens* subset) database by the Mascot search algorithm¹⁸ using trypsin (1 missed cleavages) as the digestion enzyme. The following residue modifications were allowed in the search: carbamidomethylation on cysteine and oxidation on methionine. Mascot was searched with a precursor ion tolerance of 1.0 Da and a fragment ion tolerance of 0.6 Da. Using the automatic decoy database searching tool in the Mascot, a false discovery rate for peptide matches above the identity threshold was estimated to be 4%. In addition, searches were also performed on two mgf files (one for IP lane and one for the control lane) that were generated by merging data from all the bands in each lane. The identifications from the automated search were further validated through Scaffold (Proteome Software, Portland, OR) and manual inspection of the raw data. Peptide identifications were accepted if they could be established at greater than 95% probability as specified by the Peptide Prophet algorithm¹⁹. Protein identifications were accepted if they could be established at greater than 99% probability and contained at least 2 identified peptides. Protein probabilities were assigned by the Protein Prophet algorithm²⁰.

Results

Identification of the TDP-43 interacting proteins in HEK-293 cells

TDP-43 interacting proteins in human epithelial kidney (HEK-293T) cells were isolated by immunoprecipitation of FLAG-TDP-43 followed by identification of co-purified proteins by mass spectrometry (Figure 1A, Sup. Figure 1). We found 261 proteins to be enriched in the FLAG-TDP-43 immunoprecipitate relative to control (Table 1). Of these 261 proteins, 126 were found exclusively in association with TDP-43. Sixty-eight proteins were found to be enriched in the control relative to the immunoprecipitate indicating that our immunoprecipitation was highly specific (Supplementary Table 1).

Analysis of the TDP-43 interactors reveals extensive interaction with proteins that associate with RNA, consistent with previously described roles for TDP-43 in RNA metabolism. These include hnRNPs, RNA helicases, splicing factors, translation regulatory proteins, as well as proteins involved in mRNA transport and stability (Figure 1B and Table I). TDP-43 was found to interact with a smaller number of DNA binding proteins such as transcription factors, consistent with a previously described role for TDP-43 in transcriptional repression¹, but also interacts with DNA repair proteins such as Ku70 suggesting that TDP-43 may have roles in DNA metabolism beyond transcriptional regulation (Figure 1B and Table I). Notably, although TDP-43 is predominantly a nuclear protein, we found interaction with both cytoplasmic and nuclear proteins, as well as many proteins that are known to shuttle between the nucleus and cytoplasm. This likely reflects a functional role for TDP-43 in both the nucleus and the cytoplasm consistent with the observation that TDP-43 itself undergoes nucleocytoplasmic shuttling¹².

TDP-43 associates with two distinct protein interaction networks

To gain a better understanding of the relationships between TDP-43 interacting proteins, we employed the STRING interaction database²¹. To minimize the chance of including false positives, our analysis included only those proteins in which the spectral count was at least two-fold enriched in the TDP-43 immunoprecipitate relative to control. Furthermore, only high confidence interactions as determined by the STRING database were accepted. This analysis reveals that TDP-43 interactors cluster largely into two distinct protein interaction networks (Figure 2). The “Nuclear/Splicing Cluster” is comprised entirely of nuclear proteins including many hnRNPs, but also serine/arginine-rich (SR) proteins, small nuclear ribonucleoproteins (snRNPs), an ATP-dependent RNA helicase, and nuclear RNA export factors. These proteins are all involved in nuclear RNA metabolism, primarily RNA splicing but also export of mRNA to the cytoplasm (Table 2). The “Cytoplasmic/Translation Cluster” is comprised entirely of cytoplasmic proteins, including translation initiation and elongation factors, and ribosomal subunits (Table 3). Interestingly, PABPC1 was found to link these two distinct protein interaction networks (Figure 2).

Disease-associated TDP-43 mutations do not significantly impact TDP-43 interactions

The missense mutations A315T and M337V are causative of dominantly inherited ALS^{5, 7}. To investigate whether disease-associated mutations alter the complement of proteins that interact with TDP-43, we introduced each of these mutations into TDP-43 by site-directed mutagenesis and examined their interaction profiles. We found that TDP-43 variants harboring either the A315T or M337V mutation have interaction profiles that are qualitatively indistinguishable from that of wild type TDP-43 by examination of Sypro-Ruby-stained gel (Figure 3A). This finding suggests that the mechanism by which TDP-43 missense mutants are pathogenic may be due to cell type-specific interactions that do not occur in 293T cells or that disease-causing mutations do not grossly alter the function of TDP-43 or its binding partners.

Some TDP-43 interactions are RNA-dependent whereas others are RNA-independent

Since TDP-43 and many of its interacting proteins are RNA binding proteins, we sought to determine how RNA binding influences the TDP-43 interactome. RNA binding by TDP-43 is mediated by its first RRM domain²². Two specific point mutations, W113A and R151A, have been previously shown to abolish RNA binding by TDP-43²². We introduced both of these mutations into FLAG-TDP-43 to generate the RNA binding mutant FLAG-TDP-43 (mutRRM). In comparison with FLAG-TDP-43, some TDP-43 interactions are lost with FLAG-TDP-43(mutRRM) indicating that many TDP-43 interacting proteins/complexes are strongly influenced by RNA binding (Figure 3B, lane 4). To further examine the role of RNA binding in determining TDP-43 interactions, we performed immunoprecipitation of TDP-43 in the presence of RNase A to degrade RNA. This approach yielded an almost identical interaction profile to FLAG-TDP-43(mutRRM), further demonstrating the strong influence of RNA binding on TDP-43 interactions (Figure 3B, lane 3). Many of the RNA-dependent interactions are proteins with molecular weights between ~14 and 35 kDa, a cohort largely comprised of ribosomal subunits, which suggests that the association of TDP-43 with ribosomes is indirect and mediated by interaction with the same transcript. However, other proteins are likely to interact with TDP-43 independent of its ability to bind RNA. Such proteins are more likely to be present in a multimeric protein complex with TDP-43.

Verification of TDP-43 interacting proteins

We verified a subset of TDP-43 interacting proteins by co-immunoprecipitation followed by Western blot. hnRNP H is one of a large number of hnRNPs found to interact with TDP-43 in our proteomic analysis. Similar to TDP-43, this protein has been shown to be involved in the

regulation of splicing²³. Immunoprecipitation followed by Western blot confirms an interaction between TDP-43 and hnRNP H (Figure 4A). This interaction is not altered in the disease-associated point mutations A315T or M337V (Figure 4A). The interaction between TDP-43 and hnRNP H is at least partially influenced by TDP-43 binding to RNA because treatment with RNase A strongly mitigates interaction (Figure 4A). Consistent with this finding, hnRNP H shows reduced interaction with the TDP-43(mutRRM) mutant (Figure 4A). To determine the subcellular compartment in which the interaction between TDP-43 and hnRNP H occurs, immunofluorescence was performed in HeLa cells to simultaneously visualize TDP-43 and hnRNP H. TDP-43 and hnRNP H both show pan-nuclear localization and are found to co-localize in nuclear puncta (Figure 4B).

Verification of the interaction between TDP-43 and PABPC1 was also performed. PABPC1 is a predominantly cytoplasmic protein that associates with and stabilizes poly(A) mRNA and is regulates RNA translation^{24, 25}. Immunoprecipitation followed by Western blot confirms that PABPC1 associates with TDP-43 and that this association is not affected by either the A315T or M337V mutation (Figure 4A). Immunoprecipitation in the presence of RNase A reveals that the association between TDP-43 and PABPC1 is also dependent upon RNA since binding is strongly mitigated by treatment with RNase A (Figure 4A). Consistent with this finding, PABPC1 shows reduced interaction with the TDP-43(mutRRM) mutant (Figure 4A). Thus, hnRNP H and PABPC1 interaction with TDP-43 is completely abolished by RNase A treatment, but only partially mitigated by selectively impairing the ability of TDP-43 to bind RNA (TDP-43-(mutRRM)). RNase A treatment is likely to completely disassemble ribonucleoprotein complexes, thus abolishing both direct and indirect interactions between TDP-43 and RNA binding proteins. On the other hand, the residual binding exhibited by TDP-43(mutRRM) indicates limited ability to associate with multimeric ribonucleoprotein complexes independent of its ability to bind RNA, although the interaction is clearly stabilized by RNA binding. Co-immunoprecipitation experiments were also performed in HeLa cells, confirming the interaction between PABPC1 and hnRNP H with TDP-43 and associated mutants (Sup. Figure 2A) and providing a second cell type in which these novel interactions are observed. Furthermore, we performed co-immunoprecipitation from mouse brain homogenate to confirm that interactions between TDP-43 and PABPC1 and hnRNP U occur with the endogenous TDP-43 protein in one tissue that is frequently affected in TDP-43-related disease (Sup Figure 2B).

TDP-43 localizes to RNA granules in the cytoplasm

Although TDP-43 is predominantly a nuclear protein, in some HeLa cells TDP-43 can be visualized in discrete cytoplasmic puncta in addition to diffuse nuclear staining (Figure 5A). These puncta do not stain for hnRNP H (data not shown) although they stain strongly for PABPC1, a marker for cytoplasmic RNA granules²⁶ (Figure 5A). Our findings are consistent with previous evidence indicating that TDP-43 co-purifies with cytoplasmic RNA granules²⁷. Cytoplasmic RNA granules, including stress granules, processing bodies and germ cell (or polar) granules are cytoplasmic structures believed to represent physiological accumulations of mRNA and ribonucleoproteins that modulate gene expression by influencing translation, trafficking and stability²⁸. PABPC1 is a specific marker of stress granules²⁶, suggesting that TDP-43 is present in this specific subtype of RNA granule. Further extensive evidence that TDP-43 associates with stress granules was the identification of TDP-43 interaction with numerous additional protein components of stress granules^{28, 29} (Table 4).

To confirm the association of TDP-43 with stress granules, we performed immunofluorescence to examine two additional stress granule proteins (EIF4G and G3BP1) that are also known to associate with stress granules. FLAG-TDP-43 was found to strongly co-localize with these proteins in discrete cytoplasmic puncta clearly indicating that cytoplasmic TDP-43 associates

with stress granules (Figure 5B-C). Furthermore, endogenous TDP-43 was found to localize to stress granule markers following challenge with the proteasome inhibitor MG-132, a well-established stimulus of stress granule formation (Figure 5D).

To determine whether RNA binding is necessary for TDP-43 localization to stress granules, we visualized the localization of FLAG-TDP-43(mutRRM) and EIF4G as a marker for RNA granules. The localization of FLAG-TDP-43(mutRRM) remains predominantly nuclear, although the presence of tiny discreet puncta is observed in many cells that have both nuclear and cytoplasmic localization that do not co-localize with stress granules (Figure 6). FLAG-TDP-43(mutRRM) was found to be present in only 6.5% of stress granules whereas FLAG-TDP-43 was found to be present in 84.7% of stress granules (Figure 6). This indicates that the association of TDP-43 with stress granules is strongly impaired by an inability to interact with RNA.

Discussion

Using a global proteomic approach we have demonstrated that TDP-43 has extensive interaction with proteins that regulate mRNA metabolism. These include nuclear proteins, cytoplasmic proteins, and proteins known to undergo nucleocytoplasmic shuttling. Among TDP-43's interactors are hnRNPs, RNA helicases, splicing factors, translation regulatory proteins, as well as proteins involved in mRNA transport and stability. TDP-43 was found to interact with a smaller number of DNA binding proteins such as transcription factors, consistent with a previously described role for TDP-43 in transcriptional repression¹, but also interactions with DNA repair proteins such as Ku70 suggesting that TDP-43 may be involved in other aspects of DNA metabolism.

Disease-associated mutations in TDP-43 are nearly all located within a C-terminal glycine-rich domain that has previously been found to interact with some hnRNPs^{5-9,11}. Surprisingly, the disease-causing mutations A315T and M337V do not alter the profile of TDP-43 interactions in 293T cells. Analysis using the STRING database of protein-protein interactions demonstrates that TDP-43 associates with two distinct protein interaction networks. The first is a network of nuclear proteins that regulate RNA splicing and other aspects of nuclear RNA metabolism, consistent with prior evidence that TDP-43 can influence transcription and RNA splicing¹⁰. The second is a network of cytoplasmic proteins that regulate mRNA translation. Although a predominantly nuclear protein, it has been previously shown that TDP-43 shuttles between the nucleus and cytoplasm¹². Moreover, TDP-43 has been found to redistribute to cytoplasmic RNA granules in response to neuronal injury^{13, 14}. This is consistent with our finding that TDP-43 has extensive interaction with components of stress granules and that TDP-43 colocalizes with stress granules.

TDP-43 is a relatively new player in a growing list of RNA binding proteins that are associated with disease³⁰. In addition to TDP-43, there are at least two other RNA binding proteins in which mutations lead to motor neuron disease. Loss of function mutations affecting the SMN gene cause spinal muscular atrophy³¹ whereas mutation in the SR protein FUS/TLS also leads to dominantly inherited ALS^{32, 33}. Furthermore, a large number of additional neurodegenerative diseases are also associated with mutations in RNA binding proteins indicating that defects in RNA metabolism may be a common underlying mechanism causing neurodegeneration³⁰. Our work suggests that TDP-43 may play a role in regulation of mRNA at multiple levels that may include transcription, stability, trafficking and translation. Other RNA binding proteins mutated in neurodegenerative disease are similarly multifunctional, including SMN, FUS/TLS, and FMRP. It remains to be determined whether any one particular aspect of RNA metabolism is perturbed in common amongst these diseases.

TDP-43 has a well described role in the nucleus in the negative regulation of splicing, specifically it has been shown to promote exon skipping by direct interaction with the CFTR mRNA³⁴. In the cytoplasm, TDP-43 has been shown to stabilize the mRNA of the neurofilament light chain through direct interaction with mRNA¹⁷. Recently, it has been shown that TDP-43 interacts with 14-3-3 protein subunits (also identified in our screen) to modulate the stability of the NFL mRNA³⁵. Another intriguing possibility is that TDP-43 is required for site specific translation of specific mRNAs. Previous work has shown localization of TDP-43 in RNA granules in the dendrites of hippocampal neurons and repression of translation *in vitro*³⁶. Altered regulation of site specific translation of mRNAs in motor neurons may prove to be an important mechanism leading to development of TDP-43 proteinopathies. Thus, future studies will be required to determine specific mRNAs that associate with TDP-43 in neurons.

TDP-43 pathology in ALS, FTLT-DTP and IBMPFD is typically characterized by clearance of TDP-43 from the nucleus and accumulation in the cytoplasm of affected cells². Thus, diseases mediated by TDP-43 could involve loss of TDP-43 nuclear function or gain of a toxic of function in the cytoplasm. Given the dominant mode of inheritance of ALS associated with TDP-43 mutations⁵⁻⁷, and insight derived from our *Drosophila* model of TDP-43-related disease (Ritson et al. submitted) we hypothesize that toxic gain of cytoplasmic function is more likely.

Conclusion

TDP-43 associates with two distinct protein interaction networks, one implicated in RNA metabolism nucleus and the other involved in mRNA metabolism in the cytoplasm. Many of these interactions are dependent upon the ability of TDP-43 to bind RNA. TDP-43 interactions are not altered by two mutations that are causative of ALS. The association of TDP-43 with translational machinery, as well as histological evidence of TDP-43 association with stress granules, strongly suggests that TDP-43 plays a role in translational regulation.

Supplementary Material

Refer to Web version on PubMed Central for supplementary material.

Acknowledgments

The authors thank members of the Taylor lab, particularly Natalia Nedelsky, for helpful discussion and advice. This work was supported by NIH grant AG031587 and a grant from the Packard Foundation for ALS Research at Johns Hopkins to JPT.

References

1. Ou SH, Wu F, Harrich D, Garcia-Martinez LF, Gaynor RB. Cloning and characterization of a novel cellular protein, TDP-43, that binds to human immunodeficiency virus type 1 TAR DNA sequence motifs. *J Virol* 1995;69(6):3584–96. [PubMed: 7745706]
2. Neumann M, Sampathu DM, Kwong LK, Truax AC, Micsenyi MC, Chou TT, Bruce J, Schuck T, Grossman M, Clark CM, McCluskey LF, Miller BL, Masliah E, Mackenzie IR, Feldman H, Feiden W, Kretzschmar HA, Trojanowski JQ, Lee VM. Ubiquitinated TDP-43 in frontotemporal lobar degeneration and amyotrophic lateral sclerosis. *Science* 2006;314(5796):130–3. [PubMed: 17023659]
3. Neumann M, Mackenzie IR, Cairns NJ, Boyer PJ, Markesbery WR, Smith CD, Taylor JP, Kretzschmar HA, Kimonis VE, Forman MS. TDP-43 in the ubiquitin pathology of frontotemporal dementia with VCP gene mutations. *J Neuropathol Exp Neurol* 2007;66(2):152–7. [PubMed: 17279000]
4. Geser F, Martinez-Lage M, Kwong LK, Lee VM, Trojanowski JQ. Amyotrophic lateral sclerosis, frontotemporal dementia and beyond: the TDP-43 diseases. *J Neurol* 2009;256(8):1205–14. [PubMed: 19271105]

5. Sreedharan J, Blair IP, Tripathi VB, Hu X, Vance C, Rogelj B, Ackerley S, Durnall JC, Williams KL, Buratti E, Baralle F, de Bellerocche J, Mitchell JD, Leigh PN, Al-Chalabi A, Miller CC, Nicholson G, Shaw CE. TDP-43 mutations in familial and sporadic amyotrophic lateral sclerosis. *Science* 2008;319(5870):1668–72. [PubMed: 18309045]
6. Gitcho MA, Baloh RH, Chakraverty S, Mayo K, Norton JB, Levitch D, Hatanpaa KJ, White CL 3, Bigio EH, Caselli R, Baker M, Al-Lozi MT, Morris JC, Pestronk A, Rademakers R, Goate AM, Cairns NJ. TDP-43 A315T mutation in familial motor neuron disease. *Ann Neurol* 2008;63(4):535–8. [PubMed: 18288693]
7. Kabashi E, Valdmanis PN, Dion P, Spiegelman D, McConkey BJ, Vande Velde C, Bouchard JP, Lacomblez L, Pochigaeva K, Salachas F, Pradat PF, Camu W, Meininger V, Dupre N, Rouleau GA. TARDBP mutations in individuals with sporadic and familial amyotrophic lateral sclerosis. *Nat Genet* 2008;40(5):572–4. [PubMed: 18372902]
8. Rutherford NJ, Zhang YJ, Baker M, Gass JM, Finch NA, Xu YF, Stewart H, Kelley BJ, Kuntz K, Crook RJ, Sreedharan J, Vance C, Sorenson E, Lippa C, Bigio EH, Geschwind DH, Knopman DS, Mitsumoto H, Petersen RC, Cashman NR, Hutton M, Shaw CE, Boylan KB, Boeve B, Graff-Radford NR, Wszolek ZK, Caselli RJ, Dickson DW, Mackenzie IR, Petrucelli L, Rademakers R. Novel mutations in TARDBP (TDP-43) in patients with familial amyotrophic lateral sclerosis. *PLoS Genet* 2008;4(9):e1000193. [PubMed: 18802454]
9. Borroni B, Bonvicini C, Alberici A, Buratti E, Agosti C, Archetti S, Papetti A, Stuani C, Di Luca M, Gennarelli M, Padovani A. Mutation within TARDBP leads to Frontotemporal Dementia without motor neuron disease. *Hum Mutat.* 2009
10. Buratti E, Baralle FE. Multiple roles of TDP-43 in gene expression, splicing regulation, and human disease. *FrontBiosci* 2008;13:867–78.
11. Buratti E, Brindisi A, Giombi M, Tisminetzky S, Ayala YM, Baralle FE. TDP-43 binds heterogeneous nuclear ribonucleoprotein A/B through its C-terminal tail: an important region for the inhibition of cystic fibrosis transmembrane conductance regulator exon 9 splicing. *J Biol Chem* 2005;280(45):37572–84. [PubMed: 16157593]
12. Ayala YM, Zago P, D'Ambrogio A, Xu YF, Petrucelli L, Buratti E, Baralle FE. Structural determinants of the cellular localization and shuttling of TDP-43. *J Cell Sci* 2008;121(Pt 22):3778–85. [PubMed: 18957508]
13. Moisse K, Volkening K, Leystra-Lantz C, Welch I, Hill T, Strong MJ. Divergent patterns of cytosolic TDP-43 and neuronal progranulin expression following axotomy: implications for TDP-43 in the physiological response to neuronal injury. *Brain Res* 2009;1249:202–11. [PubMed: 19046946]
14. Moisse K, Mephram J, Volkening K, Welch I, Hill T, Strong MJ. Cytosolic TDP-43 expression following axotomy is associated with caspase 3 activation in NFL(-/-) mice: Support for a role for TDP-43 in the physiological response to neuronal injury. *Brain Res.* 2009
15. Buratti E, Baralle FE. Characterization and functional implications of the RNA binding properties of nuclear factor TDP-43, a novel splicing regulator of CFTR exon 9. *J Biol Chem* 2001;276(39):36337–43. [PubMed: 11470789]
16. Abhyankar MM, Urekar C, Reddi PP. A novel CpG-free vertebrate insulator silences the testis-specific SP-10 gene in somatic tissues: role for TDP-43 in insulator function. *J Biol Chem* 2007;282(50):36143–54. [PubMed: 17932037]
17. Strong MJ, Volkening K, Hammond R, Yang W, Strong W, Leystra-Lantz C, Shoemith C. TDP43 is a human low molecular weight neurofilament (hNFL) niRNA-binding protein. *Mol Cell Neurosci* 2007;35(2):320–7. [PubMed: 17481916]
18. Perkins DN, Pappin DJ, Creasy DM, Cottrell JS. Probability-based protein identification by searching sequence databases using mass spectrometry data. *Electrophoresis* 1999;20(18):3551–67. [PubMed: 10612281]
19. Keller A, Nesvizhskii AI, Kolker E, Aebersold R. Empirical statistical model to estimate the accuracy of peptide identifications made by MS/MS and database search. *Anal Chem* 2002;74(20):5383–92. [PubMed: 12403597]
20. Nesvizhskii AI, Keller A, Kolker E, Aebersold R. A statistical model for identifying proteins by tandem mass spectrometry. *Anal Chem* 2003;75(17):4646–58. [PubMed: 14632076]

21. Jensen LJ, Kuhn M, Stark M, Chaffron S, Creevey C, Muller J, Doerks T, Julien P, Roth A, Simonovic M, Bork P, von Mering C. STRING 8--a global view on proteins and their functional interactions in 630 organisms. *Nucleic Acids Res* 2009;37(Database issue):D412–6. [PubMed: 18940858]
22. Ayala YM, Pantano S, D'Ambrogio A, Buratti E, Brindisi A, Marchetti C, Romano M, Baralle FE. Human, *Drosophila*, and *C.elegans* TDP43: nucleic acid binding properties and splicing regulatory function. *J Mol Biol* 2005;348(3):575–88. [PubMed: 15826655]
23. Chou MY, Rooke N, Turck CW, Black DL. hnRNP H is a component of a splicing enhancer complex that activates a c-src alternative exon in neuronal cells. *Mol Cell Biol* 1999;19(1):69–77. [PubMed: 9858532]
24. Bernstein P, Peltz SW, Ross J. The poly(A)-poly(A)-binding protein complex is a major determinant of mRNA stability in vitro. *Mol Cell Biol* 1989;9(2):659–70. [PubMed: 2565532]
25. Sachs AB, Davis RW. The poly(A) binding protein is required for poly(A) shortening and 60S ribosomal subunit-dependent translation initiation. *Cell* 1989;58(5):857–67. [PubMed: 2673535]
26. Hofmann I, Casella M, Schnolzer M, Schlechter T, Spring H, Franke WW. Identification of the junctional plaque protein plakophilin 3 in cytoplasmic particles containing RNA-binding proteins and the recruitment of plakophilins 1 and 3 to stress granules. *Mol Biol Cell* 2006;17(3):1388–98. [PubMed: 16407409]
27. Elvira G, Wasiak S, Blandford V, Tong XK, Serrano A, Fan X, del Rayo Sanchez-Carbente M, Servant F, Bell AW, Boismenu D, Lacaille JC, McPherson PS, DesGroseillers L, Sossin WS. Characterization of an RNA granule from developing brain. *Mol Cell Proteomics* 2006;5(4):635–51. [PubMed: 16352523]
28. Anderson P, Kedersha N. RNA granules: post-transcriptional and epigenetic modulators of gene expression. *Nat Rev Mol Cell Biol* 2009;10(6):430–6. [PubMed: 19461665]
29. Anderson P, Kedersha N. Stress granules: the Tao of RNA triage. *Trends Biochem Sci* 2008;33(3):141–50. [PubMed: 18291657]
30. Cooper TA, Wan L, Dreyfuss G. RNA and disease. *Cell* 2009;136(4):777–93. [PubMed: 19239895]
31. Lefebvre S, Burglen L, Reboullet S, Clermont O, Burlet P, Viollet L, Benichou B, Cruaud C, Millasseau P, Zeviani M, et al. Identification and characterization of a spinal muscular atrophy-determining gene. *Cell* 1995;80(1):155–65. [PubMed: 7813012]
32. Kwiatkowski TJ Jr, Bosco DA, Leclerc AL, Tamrazian E, Vanderburg CR, Russ C, Davis A, Gilchrist J, Kasarskis EJ, Munsat T, Valdmanis P, Rouleau GA, Hosler BA, Cortelli P, de Jong PJ, Yoshinaga Y, Haines JL, Pericak-Vance MA, Yan J, Ticozzi N, Siddique T, McKenna-Yasek D, Sapp PC, Horvitz HR, Landers JE, Brown RH Jr. Mutations in the FUS/TLS gene on chromosome 16 cause familial amyotrophic lateral sclerosis. *Science* 2009;323(5918):1205–8. [PubMed: 19251627]
33. Vance C, Rogelj B, Hortobagyi T, De Vos KJ, Nishimura AL, Sreedharan J, Hu X, Smith B, Ruddy D, Wright P, Ganesalingam J, Williams KL, Tripathi V, Al-Saraj S, Al-Chalabi A, Leigh PN, Blair IP, Nicholson G, de Belleruche J, Gallo JM, Miller CC, Shaw CE. Mutations in FUS, an RNA processing protein, cause familial amyotrophic lateral sclerosis type 6. *Science* 2009;323(5918):1208–11. [PubMed: 19251628]
34. Buratti E, Dork T, Zuccato E, Pagani F, Romano M, Baralle FE. Nuclear factor TDP-43 and SR proteins promote in vitro and in vivo CFTR exon 9 skipping. *EMBO J* 2001;20(7):1774–84. [PubMed: 11285240]
35. Volkening K, Leystra-Lantz C, Yang W, Jaffee H, Strong MJ. Tar DNA binding protein of 43 kDa (TDP-43), 14-3-3 proteins and copper/zinc superoxide dismutase (SOD1) interact to modulate NFL mRNA stability. Implications for altered RNA processing in amyotrophic lateral sclerosis (ALS). *Brain Res*. 2009
36. Wang IF, Wu LS, Chang HY, Shen CK. TDP-43, the signature protein of FTLN-U, is a neuronal activity-responsive factor. *J Neurochem* 2008;105(3):797–806. [PubMed: 18088371]

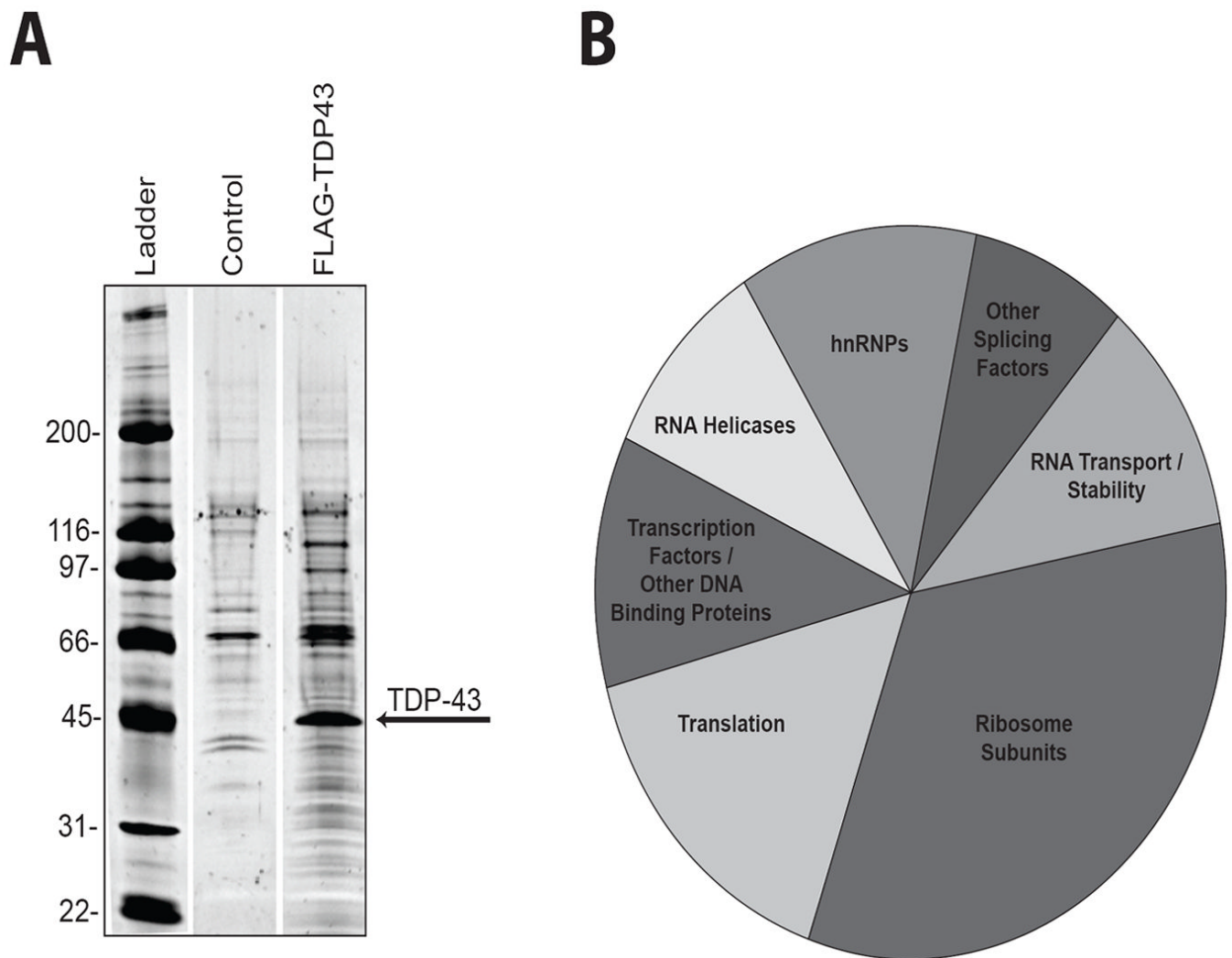


Figure 1. Identification of TDP-43 interacting proteins by FLAG-immunoprecipitation
(A) Immunoprecipitates from FLAG-TDP-43-expressing HEK-293T cells or control HEK-293T cells were separated by gel electrophoresis and stained with Sypro-Ruby to visualize proteins. Both the control and FLAG-TDP-43 lanes were separated into 24 bands along the entire length of the gel and analyzed by mass spectrometry. Intervening empty lanes were removed for visualization purposes. **(B)** Pie-chart representation of functional classes of TDP-43-interacting proteins.

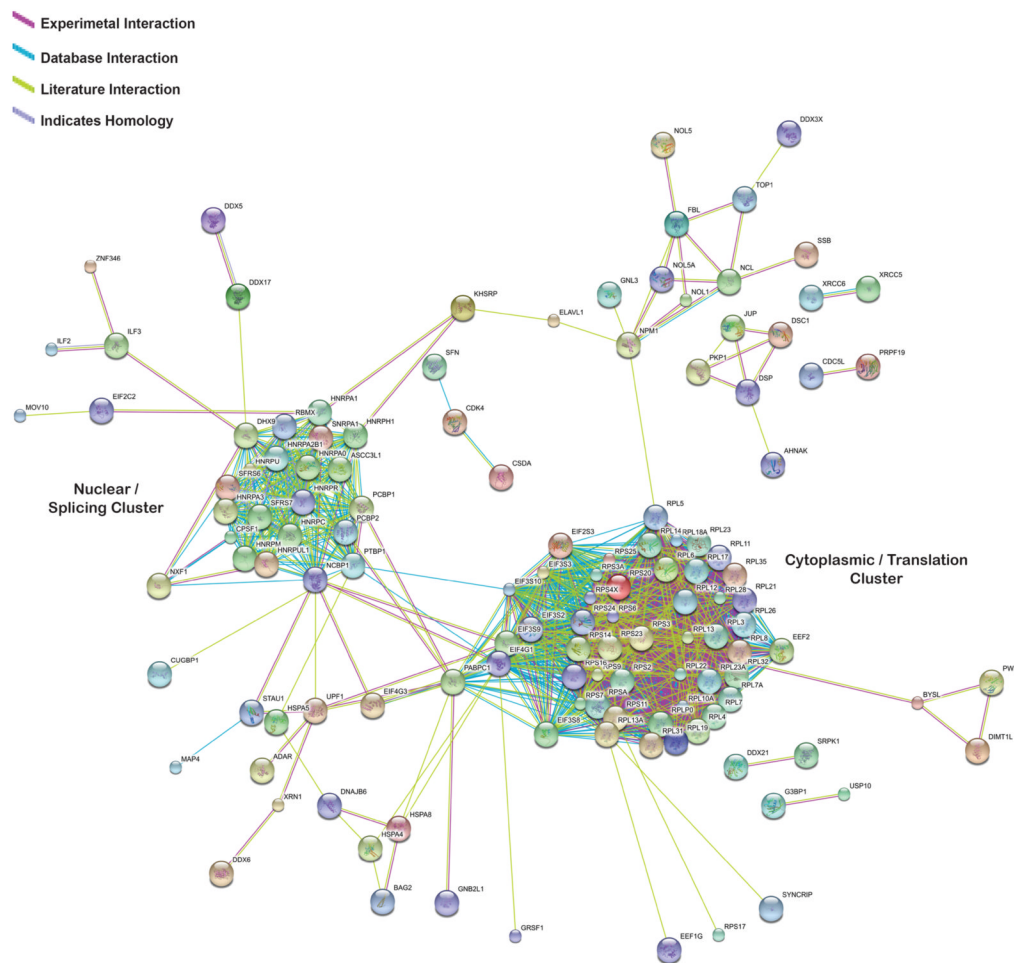


Figure 2. TDP-43 interacting proteins form two distinct protein interaction networks
 TDP-43 proteins identified by mass spectrometry were analyzed using STRING interaction software to identify high confidence interactions using database, literature, and experimental search parameters. Only proteins that were at least two-fold enriched in the TDP-43 immunoprecipitate were analyzed using STRING. Two distinct protein interactions were observed that are labeled as the Nuclear/Splicing Cluster and the Cytoplasmic/Translation Cluster.

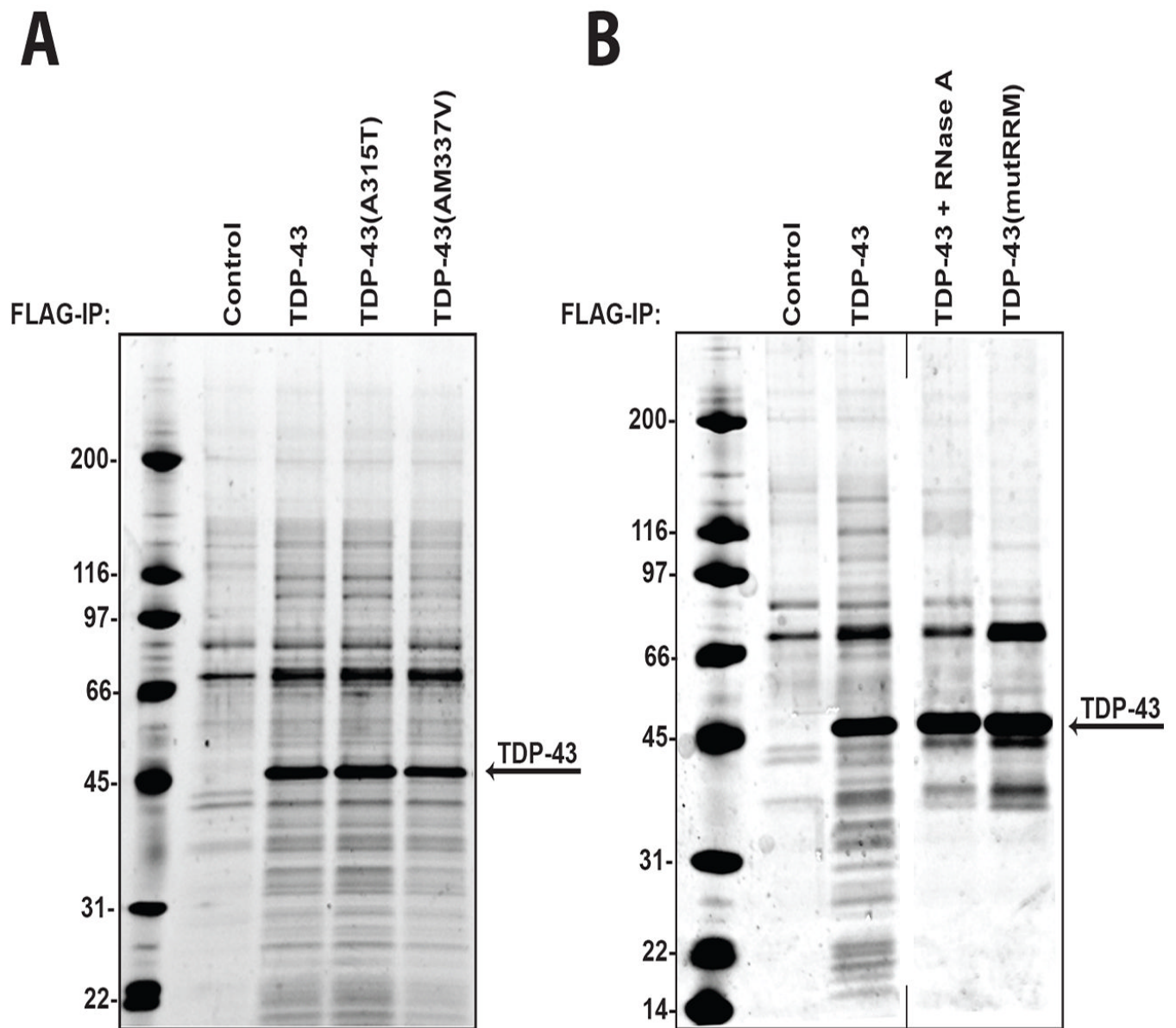
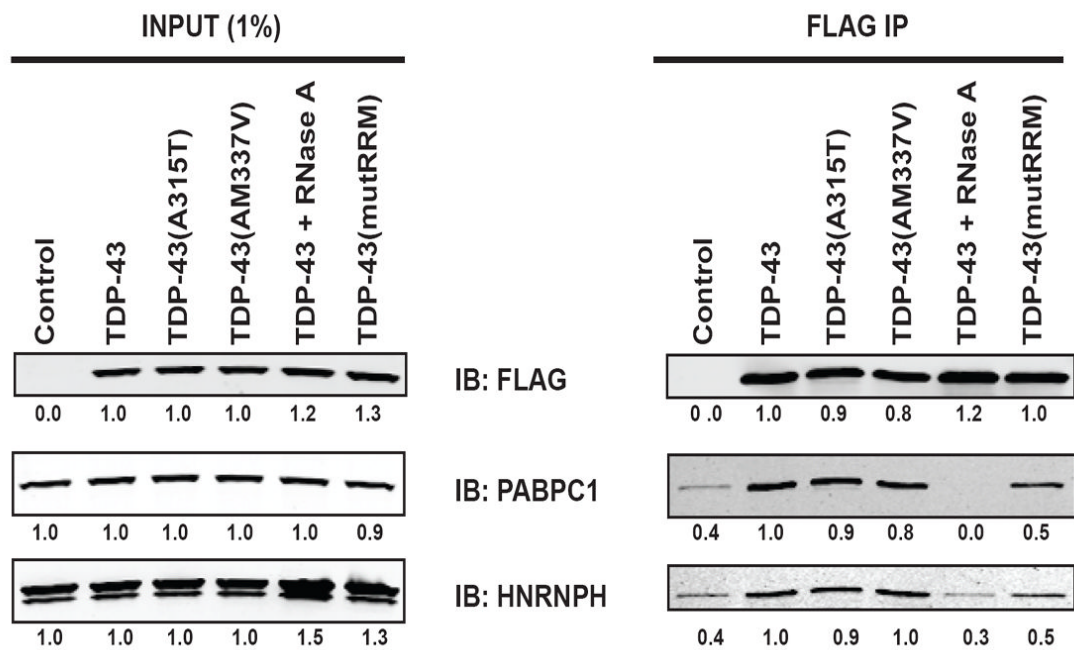
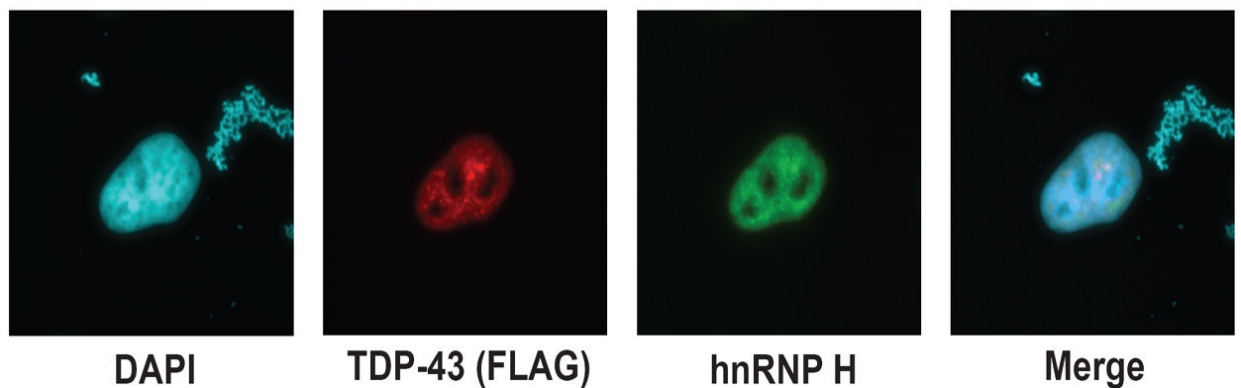


Figure 3. The impact of TDP-43 mutations on interactions

(A) Disease-associated mutations do not alter the TDP-43 interactome. The figure shows Sypro-Ruby-stained FLAG immunoprecipitates from control HEK-293T cells, HEK-293T cells expressing wild type FLAG-TDP-43, FLAG-TDP-43 (A315T) or FLAG-TDP-43 (M337V) as indicated. FLAG-TDP-43 (M337V) reproducibly immunoprecipitates less efficiently than either FLAG-TDP-43 or FLAG-TDP-43 (A315T) which is proportional to the decrease in intensity of interacting proteins as visualized by Sypro-Ruby. (B) Some TDP-43 interactions are RNA-dependent. The figure shows Sypro-Ruby-stained FLAG immunoprecipitates from control HEK-293T cells, HEK-293T cells expressing wild type FLAG-TDP-43, wild type FLAG-TDP-43 (treated with RNase A), or FLAG-TDP-43 (mutRRM), as indicated. Immunoprecipitation was repeated at least three times with consistent results. Representative images were chosen for display.

A**B****Figure 4. Characterization of TDP-43 interaction with hnRNP H and PABPC1**

(A) Validation of TDP-43 interaction with hnRNP H and PABPC1 by co-immunoprecipitation followed by Western blot analysis in HEK-293T cells. Left panel: Western blot analysis of whole cell lysates prior to immunoprecipitation was used to visualize 1% of protein input. Right panel: Western blot analysis of FLAG immunoprecipitates. Quantification was performed using Image J (shown below each band) and normalized to the amount of TDP-43 in lane 2. Immunoprecipitation was repeated at least three times with consistent results and representative images were chosen for display. (B) Immunofluorescence was used to visualize the localization of TDP-43 and hnRNP H in HeLa cells. DAPI staining was used to visualize the nucleus. TDP-43 and hnRNP H both showed pan-nuclear expression with co-localization

in sub-nuclear foci in HeLa cells. The immunofluorescence data shown represents consistent results obtained in multiple replicates. IB: immunoblot, IP: immunoprecipitation.

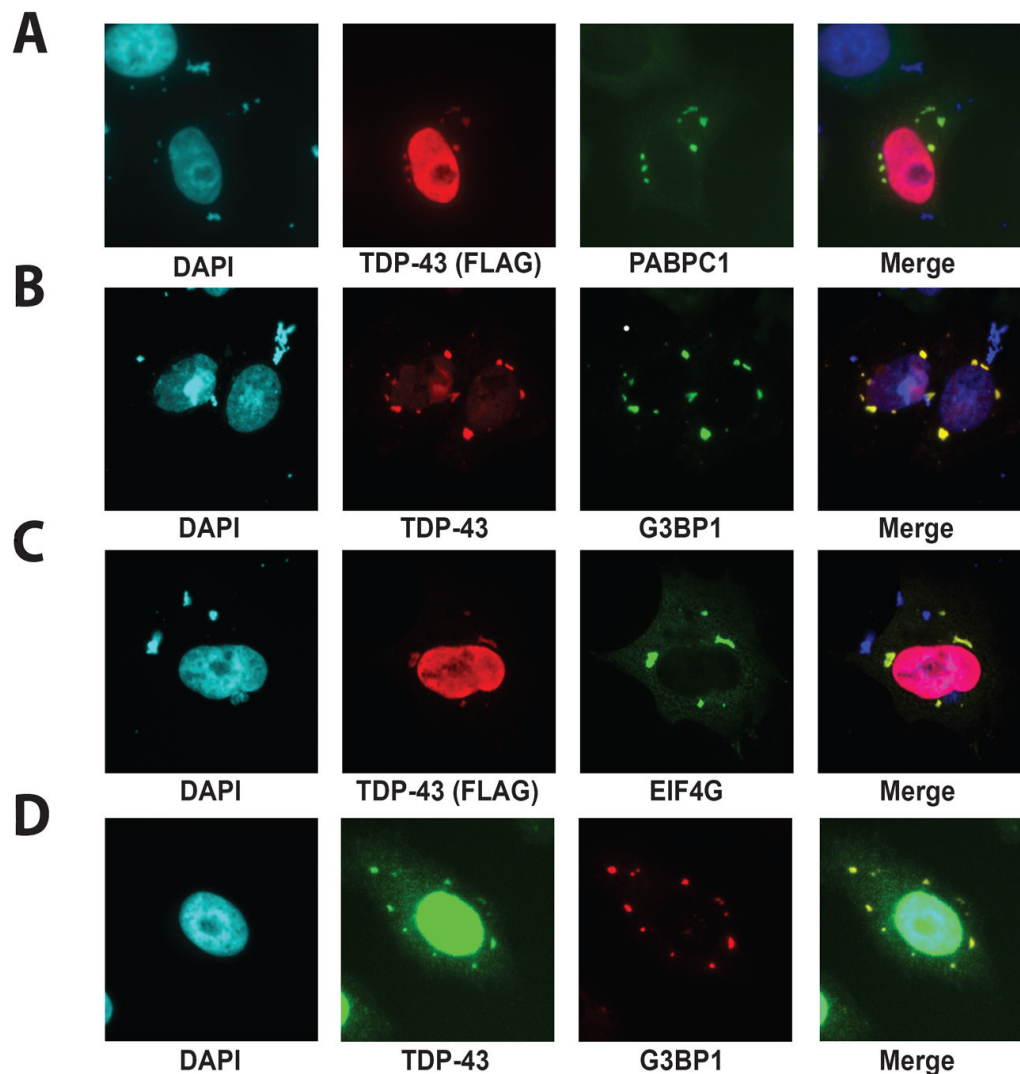


Figure 5. Cytoplasmic TDP-43 is localized in stress granules

Immunofluorescence was used to visualize the localization of exogenous (A-C) FLAG-TDP-43 or endogenous (D) TDP-43 and (A) PABPC1, (B, D) G3BP1 and (C) EIF4G in HeLa cells. DAPI staining was used to visualize the nucleus. TDP-43 was found to localize with stress granules in the cytoplasm of HeLa cells. (D) After treatment with 50 μ M MG-132 for 3 hours, RNA granules were observed in 66% of cells. At least 1 TDP-43 positive stress granule was observed in 25% of cells after MG-132 treatment. 300 HeLa cells were counted. All of the immunofluorescence data shown represents consistent results obtained in multiple replicates.

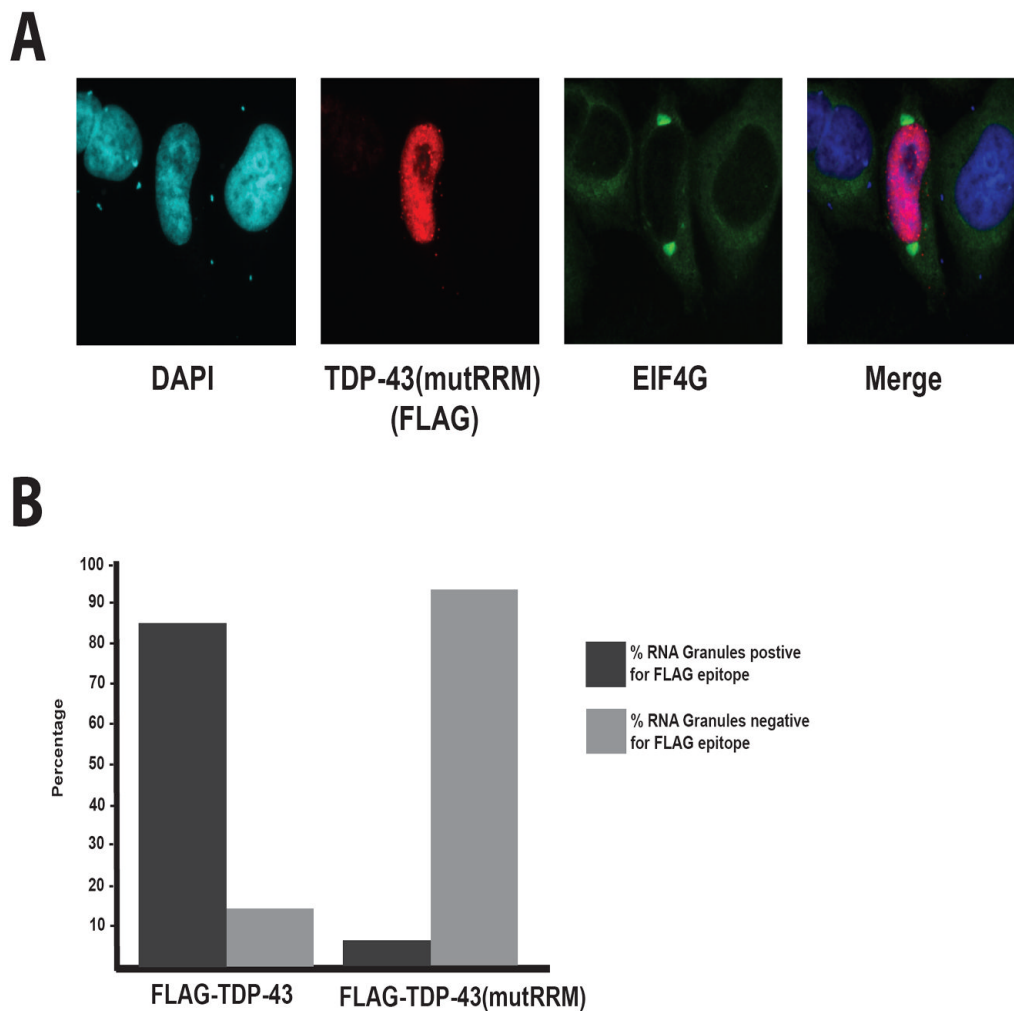


Figure 6. TDP-43 association with stress granules is strongly mitigated by inability to bind RNA (A) TDP-43(mutRRM) was rarely found in cytoplasmic RNA granules (as visualized by EIF4G). (B) In FLAG-TDP-43 expressing cells, FLAG-TDP-43 was found to co-localize with EIF4G in 85% of stress granules (n=242 cells) whereas FLAG-TDP-43(mutRRM) was found in only 6.5% of stress granules (n=168 cells).

TDP-43 Interacting Proteins**Table 1**

Proteins identified by mass spectrometry that were enriched in TDP-43 immunoprecipitation compared to control. Protein symbol in parenthesis is gene name assigned by STRING as used in Figure 2 if it differs from the official gene name. An asterisk in the final column indicates that no peptides were identified as being present in the control lane.

Protein Name	Symbol	Molecular Weight (kDa)	Accession Number	Total Spectra: FLAG IP	Unique Peptides: FLAG IP	Percent Coverage: FLAG IP	Total Spectra: Control	Unique Peptides: Control	Percent Coverage: Control	Fold Spectra Increase: IP / Control
TAR DNA-binding protein 43	TARDBP	45	Q13148	176	17	35	0	0	0	*
40S ribosomal protein S3	RPS3	27	P23396	68	16	55	22	10	47	3.1
Nucleolin	NCL	77	P19338	57	20	25	19	8	11	3.0
Polyadenylate-binding protein 1	PABPC1	71	P11940	53	27	36	27	16	25	2.0
Heat shock cognate 71 kDa protein	HSPA8	71	P11142	51	23	33	13	7	14	3.9
ATP-dependent RNA helicase A	DHX9	141	Q08211	49	27	23	14	12	10	3.5
Histone H1.3	HIST1H1D	22	P16402	46	7	19	5	3	15	9.2
Heat shock 70 kDa protein 1	HSPA1A	70	P08107	44	23	28	14	10	17	3.1
Heterogeneous nuclear ribonucleoprotein U	HNRNPU (HNRPU)	91	Q00839	43	16	17	15	8	9	2.9
Interleukin enhancer-binding factor 3	ILF3	95	Q12906	42	14	17	10	5	7	4.2
Putative ATP-dependent RNA helicase DHX30	DHX30	134	Q7L2E3	41	24	18	2	2	2	20.5
40S ribosomal protein S9	RPS9	23	P46781	40	15	46	9	3	9	4.4
60S ribosomal protein L7a	RPL7A	30	P62424	38	12	35	11	3	9	3.5
Heterogeneous nuclear ribonucleoproteins A2/B1	HNRNPA2B1 (HNRPA2B1)	37	P22626	38	9	24	13	5	17	2.9
Heterogeneous nuclear ribonucleoproteins C1/C2	HNRNPC (HNRPC)	34	P07910	34	12	28	6	5	19	5.7
Insulin-like growth factor 2 mRNA-binding protein 1	IGF2BP1	63	Q9NZ18	33	17	31	20	13	27	1.7
Probable ATP-dependent RNA helicase DDX5	DDX5	69	P17844	32	15	27	8	5	9	4.0
40S ribosomal protein S18	RPS18	18	P62269	31	11	49	5	3	19	6.2
40S ribosomal protein SA	RPSA	33	P08865	30	12	42	7	3	13	4.3
60S ribosomal protein L6	RPL6	33	Q02878	30	9	29	3	3	9	10.0
Nucleolar RNA helicase 2	DDX21	87	Q9NR30	29	16	20	0	0	0	*
RNA-binding protein Musashi homolog 2	MSI2	35	Q96DH6	29	5	21	0	0	0	*

Protein Name	Symbol	Molecular Weight (kDa)	Accession Number	Total Spectra: FLAG IP	Unique Peptides: FLAG IP	Percent Coverage: FLAG IP	Total Spectra: Control	Unique Peptides: Control	Percent Coverage: Control	Fold Spectra Increase: IP / Control
Trypsin-3	PRSS3	33	P35030	29	3	10	18	2	7	1.6
La-related protein 1	LARP1	124	Q6PKG0	27	11	9	4	3	4	6.8
Heterogeneous nuclear ribonucleoprotein A1	HNRNPA1 (HNRPA1)	39	P09651	27	8	25	8	5	18	3.4
Putative helicase MOV-10	MOV10	114	Q9HCE1	26	18	21	7	6	8	3.7
Regulator of nonsense transcripts 1	UPF1	124	Q92900	25	18	14	2	2	2	12.5
Tubulin beta chain	TUBB	50	P07437	25	8	20	12	7	19	2.1
40S ribosomal protein S3a	RPS3A	30	P61247	24	11	36	4	3	10	6.0
Probable ATP-dependent RNA helicase DDX17	DDX17	72	Q92841	23	11	20	1	1	2	23.0
40S ribosomal protein S16	RPS16	16	P62249	23	7	42	4	3	19	5.8
Heterogeneous nuclear ribonucleoprotein Q	SYNCRIP	70	O60506	23	9	15	8	6	7	2.9
Heterogeneous nuclear ribonucleoprotein K	HNRNPK	51	P61978	23	10	25	19	11	28	1.2
40S ribosomal protein S2	RPS2	31	P15880	22	9	27	2	2	7	11.0
Heterogeneous nuclear ribonucleoprotein M	HNRNPM (HNRPM)	78	P52272	22	13	24	3	3	5	7.3
ATP-dependent DNA helicase 2 subunit 1	XRCC6	70	P12956	21	12	17	0	0	0	*
40S ribosomal protein S6	RPS6	29	P62753	21	7	17	2	1	3	10.5
Heterogeneous nuclear ribonucleoprotein U-like protein 1	HNRNPUL1 (HNRPUL1)	96	Q9BUJ2	21	9	13	1	1	2	21.0
60S acidic ribosomal protein P0	RPLP0	34	P05388	21	12	47	4	3	10	5.3
60S ribosomal protein L26	RPL26	17	P61254	20	6	29	2	1	6	10.0
60S ribosomal protein L8	RPL8	28	P62917	20	6	19	3	1	4	6.7
40S ribosomal protein S4, X isoform	RPS4X	30	P62701	20	12	46	7	4	17	2.9
Zinc finger CCHH-type antiviral protein 1	ZC3HAV1	101	Q7Z2W4	19	12	14	0	0	0	*
Ubiquitin	RPS27A (UBB)	9	P61864	19	3	45	8	2	33	2.4
Heterogeneous nuclear ribonucleoprotein D0	HNRNPD	38	Q14103	19	7	25	10	3	9	1.9
Poly(rC)-binding protein 2	PCBP2	39	Q15366	19	7	25	9	5	19	2.1

Protein Name	Symbol	Molecular Weight (kDa)	Accession Number	Total Spectra: FLAG IP	Unique Peptides: FLAG IP	Percent Coverage: FLAG IP	Total Spectra: Control	Unique Peptides: Control	Percent Coverage: Control	Fold Spectra Increase: IP / Control
ATP-dependent RNA helicase DDX1	DDX1	82	Q92499	19	10	15	15	7	10	1.3
BAT2 domain-containing protein 1	BAT2D1	317	Q9Y520	18	9	3	0	0	0	*
60S ribosomal protein L7	RPL7	29	P18124	18	7	16	4	1	4	4.5
Probable ATP-dependent RNA helicase DHX36	DHX36	115	Q9H2U1	18	11	11	1	1	1	18.0
DNA-binding protein A	CSDA	40	P16989	18	8	24	5	2	10	3.6
Polyadenylate-binding protein 4	PABPC4	71	Q13310	18	14	16	2	2	3	9.0
60S ribosomal protein L13	RPL13	24	P26373	18	6	27	8	5	21	2.3
Splicing factor, proline- and glutamine-rich	SFPQ	76	P23246	18	11	16	10	7	10	1.8
Insulin-like growth factor 2 mRNA-binding protein 3	IGF2BP3	64	O00425	18	12	23	14	10	16	1.3
Eukaryotic translation initiation factor 4 gamma 1	EIF4G1	176	Q04637	17	10	7	0	0	0	*
Nucleophosmin	NPM1	33	P06748	17	6	26	2	1	3	8.5
60S ribosomal protein L4	RPL4	48	P36578	17	7	19	2	2	5	8.5
Heterogeneous nuclear ribonucleoprotein H	HNRNPH1 (HNRNPH1)	49	P31943	17	7	22	4	2	6	4.3
DNA topoisomerase 1	TOP1	91	P11387	16	10	13	0	0	0	*
La-related protein 4	LARP4	81	Q71RC2	16	9	16	0	0	0	*
40S ribosomal protein S25	RPS25	14	P62851	16	4	24	7	3	24	2.3
60S ribosomal protein L18	RPL18	22	Q07020	16	6	31	15	4	25	1.1
40S ribosomal protein S11	RPS11	18	P62280	15	9	48	0	0	0	*
40S ribosomal protein S14	RPS14	16	P62263	15	6	25	2	1	7	7.5
Serine/threonine-protein kinase 38	STK38	54	Q15208	15	6	13	12	7	14	1.3
60 kDa heat shock protein, mitochondrial	HSPD1	61	P10809	15	10	17	10	8	15	1.5
Matrin-3	MATR3	95	P43243	14	9	10	0	0	0	*
Probable ATP-dependent RNA helicase YTHDC2	YTHDC2	160	Q9H6S0	14	6	5	0	0	0	*
Non-POU domain-containing octamer-binding protein	NONO	54	Q15233	14	9	25	12	7	22	1.2
ELAV-like protein 1	ELAVL1	36	Q15717	13	5	15	4	2	7	3.3

Protein Name	Symbol	Molecular Weight (kDa)	Accession Number	Total Spectra: FLAG IP	Unique Peptides: FLAG IP	Percent Coverage: FLAG IP	Total Spectra: Control	Unique Peptides: Control	Percent Coverage: Control	Fold Spectra Increase: IP / Control
Far upstream element-binding protein 2	KHSRP	73	Q92945	13	9	16	2	2	3	6.5
Tubulin alpha-1B chain	TUBA1B	50	P68363	13	9	26	4	3	9	3.3
Microtubule-associated protein 1B	MAP1B	271	P46821	13	12	6	10	10	5	1.3
Dermcidin	DCD	11	P81605	12	2	20	0	0	0	*
Heterogeneous nuclear ribonucleoprotein A/B	HNRNPAB	36	Q99729	12	5	13	0	0	0	*
Insulin-like growth factor 2 mRNA-binding protein 2	IGF2BP2	66	Q9Y6M1	12	8	17	1	1	2	12.0
Constitutive coactivator of PPAR-gamma-like protein 1	FAM120A	122	Q9NZB2	12	6	8	3	2	2	4.0
Ras GTPase-activating protein-binding protein 1	G3BP1	52	Q13283	12	5	13	2	2	6	6.0
Caprin-1	CAPRIN1	78	Q14444	12	5	8	5	3	4	2.4
Interleukin enhancer-binding factor 2	ILF2	43	Q12905	12	7	21	4	3	9	3.0
Heat shock protein 105 kDa	HSPH1	97	Q92598	11	7	10	0	0	0	*
Heterogeneous nuclear ribonucleoprotein U-like protein 2	HNRNPUL2	85	Q1KMD3	11	8	12	0	0	0	*
Lupus La protein	SSB	47	P05455	11	5	11	0	0	0	*
Probable dimethyladenosine transferase	DIMT1L	35	Q9UNQ2	11	7	27	0	0	0	*
Heterogeneous nuclear ribonucleoprotein A3	HNRNPA3 (HNRNPA3)	40	P51991	11	8	19	1	1	3	11.0
Polypyrimidine tract-binding protein 1	PTBP1	57	P26599	11	4	6	1	1	2	11.0
60S ribosomal protein L3	RPL3	46	P39023	11	7	21	3	2	6	3.7
40S ribosomal protein S19	RPS19	16	P39019	11	4	18	7	3	13	1.6
60S ribosomal protein L5	RPL5	34	P46777	10	7	25	0	0	0	*
RNA-binding protein Musashi homolog 1	MSH1	39	O43347	10	5	18	0	0	0	*
60S ribosomal protein L10	RPL10	25	P27635	10	6	21	4	3	17	2.5
UPP0027 protein C22orf28	C22orf28	55	Q9Y310	10	7	14	6	5	10	1.7
14-3-3 protein sigma	SFN	28	P31947	9	6	19	0	0	0	*
Double-stranded RNA-binding protein Staufen homolog 1	STAU1	63	O95793	9	6	12	0	0	0	*
La-related protein 4B	LARP4B	81	A6NEL6	9	5	7	0	0	0	*

Protein Name	Symbol	Molecular Weight (kDa)	Accession Number	Total Spectra: FLAG IP	Unique Peptides: FLAG IP	Percent Coverage: FLAG IP	Total Spectra: Control	Unique Peptides: Control	Percent Coverage: Control	Fold Spectra Increase: IP / Control
40S ribosomal protein S20	RPS20	13	P60866	9	6	29	1	1	9	9.0
60S ribosomal protein L12	RPL12	18	P30050	9	6	43	2	1	6	4.5
60S ribosomal protein L19	RPL19	23	P84098	9	4	10	3	1	5	3.0
ATP-dependent RNA helicase DDX3X	DDX3X	73	O00571	9	7	12	2	1	2	4.5
Splicing factor, arginine/serine-rich 7	SFRS7	27	Q16629	9	3	15	2	1	4	4.5
60S ribosomal protein L24	RPL24	18	P83731	9	3	18	5	2	13	1.8
ADP/ATP translocase 2	SLC25A5	33	P05141	9	7	20	2	2	8	4.5
ATP-dependent DNA helicase 2 subunit 2	XRCC5	83	P13010	8	5	7	0	0	0	*
Histone H1x	H1FX	22	Q92522	8	4	18	0	0	0	*
Probable helicase with zinc finger domain	HELZ	219	P42694	8	6	4	0	0	0	*
Putative ATP-dependent RNA helicase DHX57	DHX57	156	Q6P158	8	5	4	0	0	0	*
60S ribosomal protein L31	RPL31	14	P62899	8	2	15	3	1	7	2.7
60S ribosomal protein L35	RPL35	15	P42766	8	2	19	4	1	8	2.0
Heat shock 70 kDa protein 4	HSPA4	94	P34932	8	6	9	1	1	2	8.0
60S ribosomal protein L14	RPL14	23	P50914	8	6	24	2	2	11	4.0
Elongation factor 2	EEF2	95	P13639	8	5	7	3	2	2	2.7
Heterogeneous nuclear ribonucleoprotein G	RBMX	42	P38159	8	5	14	3	2	6	2.7
Nuclease-sensitive element-binding protein 1	YBX1	36	P67809	8	2	12	5	3	19	1.6
40S ribosomal protein S7	RPS7	22	P62081	7	5	23	0	0	0	*
Far upstream element-binding protein 3	FUBP3	62	Q96124	7	6	12	0	0	0	*
Guanine nucleotide-binding protein-like 3	GNL3	62	Q9BVP2	7	5	12	0	0	0	*
Heterogeneous nuclear ribonucleoprotein R	HNRNPR (HNRPR)	71	O43390	7	4	8	0	0	0	*
Ribosome-binding protein 1	RRBP1	152	Q9P2E9	7	5	4	0	0	0	*
Serine/threonine-protein kinase SRPK1	SRPK1	74	Q96SB4	7	4	7	0	0	0	*
Splicing factor, arginine/serine-rich 6	SFRS6	40	Q13247	7	2	5	0	0	0	*
Transcription intermediary factor 1-beta	TRIM28	89	Q13263	7	5	7	0	0	0	*

Protein Name	Symbol	Molecular Weight (kDa)	Accession Number	Total Spectra: FLAG IP	Unique Peptides: FLAG IP	Percent Coverage: FLAG IP	Total Spectra: Control	Unique Peptides: Control	Percent Coverage: Control	Fold Spectra Increase: IP / Control
Desmoplakin	DSP	332	P15924	7	6	2	1	1	0	7.0
60S ribosomal protein L23a	RPL23A	18	P62750	7	5	28	3	2	15	2.3
Junction plakoglobin	JUP	82	P14923	7	7	9	3	3	5	2.3
Heterogeneous nuclear ribonucleoprotein L	HNRNPL	64	P14866	7	5	10	4	4	7	1.8
ATP-dependent RNA helicase DDX50	DDX50	83	Q9BQ39	6	4	6	0	0	0	*
Bystin	BYSL	50	P48634	6	6	18	0	0	0	*
Nuclear fragile X mental retardation-interacting protein 2	NUFIP2	76	Q7Z417	6	4	7	0	0	0	*
Plakophilin-1	PKP1	83	Q13835	6	4	6	0	0	0	*
Plasminogen activator inhibitor 1 RNA-binding protein	SERBP1	45	Q8NC51	6	6	15	0	0	0	*
Protein LYRIC	MTDH	64	Q86UE4	6	5	11	0	0	0	*
Serrate RNA effector molecule homolog	SRRT	101	Q9BXP5	6	4	5	0	0	0	*
U5 small nuclear ribonucleoprotein 200 kDa helicase	SNRNP200 (ASCC3L1)	245	O75643	6	6	3	0	0	0	*
Zinc finger RNA-binding protein	ZFR	117	Q96KR1	6	5	7	0	0	0	*
40S ribosomal protein S5	RPS5	23	P46782	6	3	12	4	1	4	1.5
60S ribosomal protein L10a	RPL10A	25	P62906	6	4	13	2	1	4	3.0
60S ribosomal protein L23	RPL23	15	P62829	6	3	32	2	1	11	3.0
78 kDa glucose-regulated protein	HSPA5	72	P11021	6	5	11	1	1	2	6.0
Heterogeneous nuclear ribonucleoprotein A0	HNRNPA0 (HNRPA0)	31	Q13151	6	2	12	1	1	5	6.0
Serum albumin	ALB	69	P02768	6	2	4	5	1	3	1.2
Ras GTPase-activating protein-binding protein 2	G3BP2	54	Q9UN86	6	4	12	2	2	5	3.0
Methylosome subunit p1Cln	CLNS1A	26	P54105	6	5	32	5	3	19	1.2
U2 small nuclear ribonucleoprotein A'	SNRPA1	28	P09661	6	4	18	3	3	15	2.0
40S ribosomal protein S23	RPS23	16	P62266	5	2	16	0	0	0	*
60S ribosomal protein L17	RPL17	21	P18621	5	3	13	0	0	0	*
60S ribosomal protein L28	RPL28	16	P46779	5	4	27	0	0	0	*
60S ribosomal protein L9	RPL9	22	P32969	5	4	22	0	0	0	*

Protein Name	Symbol	Molecular Weight (kDa)	Accession Number	Total Spectra: FLAG IP	Unique Peptides: FLAG IP	Percent Coverage: FLAG IP	Total Spectra: Control	Unique Peptides: Control	Percent Coverage: Control	Fold Spectra Increase: IP / Control
NF-kappa-B-repressing factor	NKRF	78	O15226	5	3	4	0	0	0	*
Nuclear RNA export factor 1	NXF1	70	Q9UBU9	5	4	7	0	0	0	*
Nucleolar protein 56	NOP56 (NOL5A)	66	O00567	5	4	7	0	0	0	*
Poly(rC)-binding protein 1	PCBP1	37	Q15365	5	3	11	0	0	0	*
Putative RNA-binding protein Luc7-like 2	LUC7L2	47	Q9Y383	5	2	6	0	0	0	*
RNA-binding protein Raly	RALY	32	Q9UKM9	5	4	17	0	0	0	*
rRNA 2'-O-methyltransferase fibrillar	FBL	34	P22087	5	4	16	0	0	0	*
YTH domain family protein 2	YTHDF2	62	Q9Y5A9	5	3	6	0	0	0	*
Eukaryotic translation initiation factor 3 subunit B	EIF3B (PRT1)	92	P55884	5	3	4	1	1	1	5.0
Eukaryotic initiation factor 4A-I	EIF4A1	46	P60842	5	4	12	3	2	6	1.7
Heterogeneous nuclear ribonucleoprotein D-like	HNRPDL	46	O14979	5	2	6	2	2	6	2.5
RING finger protein 219	RNF219	81	Q5W0B1	5	3	5	3	2	4	1.7
RNA-binding protein FUS	FUS	53	P35637	5	3	8	3	2	5	1.7
28S ribosomal protein S29, mitochondrial	DAP3	46	P51398	4	2	6	0	0	0	*
Ataxin-2-like protein	ATXN2L	113	Q8WWM7	4	4	4	0	0	0	*
Cell division cycle 5-like protein	CDC5L	92	Q99459	4	4	7	0	0	0	*
Desmocollin-1	DSC1	100	Q08554	4	2	3	0	0	0	*
DNA-directed RNA polymerase, mitochondrial	POLRMT	139	O00411	4	3	4	0	0	0	*
Double-stranded RNA-specific adenosine deaminase	ADAR	136	P55265	4	3	4	0	0	0	*
G-rich sequence factor 1	GRSF1	53	Q12849	4	2	6	0	0	0	*
Large proline-rich protein BAT2	BAT2	229	P48634	4	3	2	0	0	0	*
Nuclear cap-binding protein subunit 1	NCBP1	92	Q09161	4	3	4	0	0	0	*
Nucleolar protein 58	NOP58 (NOL5)	60	Q9Y2X3	4	4	11	0	0	0	*
Pre-rRNA-processing protein TSR1 homolog	TSR1	92	Q2NL82	4	3	4	0	0	0	*
Putative ribosomal RNA methyltransferase NOP2	NOP2 (NOL1)	89	P46087	4	4	7	0	0	0	*

Protein Name	Symbol	Molecular Weight (kDa)	Accession Number	Total Spectra: FLAG IP	Unique Peptides: FLAG IP	Percent Coverage: FLAG IP	Total Spectra: Control	Unique Peptides: Control	Percent Coverage: Control	Fold Spectra Increase: IP / Control
TRM1-like protein	TRM1L	82	Q7Z2T5	4	3	5	0	0	0	*
Ubiquitin carboxyl-terminal hydrolase 10	USP10	87	Q14694	4	2	3	0	0	0	*
60S ribosomal protein L11	RPL11	20	P62913	4	2	12	1	1	8	4.0
60S ribosomal protein L22	RPL22	15	P35268	4	2	19	2	1	10	2.0
60S ribosomal protein L27a	RPL27A	17	P46776	4	2	16	3	1	7	1.3
Eukaryotic translation initiation factor 3 subunit C	EIF3C (EIF3S8)	105	Q99613	4	4	5	1	1	2	4.0
Pre-mRNA-processing factor 19	PRPF19	55	Q9UMS4	4	3	6	2	1	2	2.0
Probable ATP-dependent RNA helicase DDX6	DDX6	54	P26196	4	3	5	1	1	5	4.0
Staphylococcal nuclease domain-containing protein 1	SND1	102	Q7KZF4	4	4	6	1	1	1	4.0
Leucine-rich repeat-containing protein 59	LRRC59	35	Q96AG4	4	2	7	3	2	7	1.3
Myosin-9	MYH9	227	P35579	4	4	2	2	2	1	2.0
Uncharacterized protein C11orf84	C11orf84	41	Q9Y520	4	3	12	3	2	5	1.3
Eukaryotic initiation factor 4A-III	EIF4A3	47	P38919	4	4	10	3	3	8	1.3
Protein FAM98B	FAM98B	37	Q9NZB2	4	3	12	3	3	12	1.3
28S ribosomal protein S27, mitochondrial	MRPS27	48	Q92552	3	2	5	0	0	0	*
39S ribosomal protein L12, mitochondrial	MRPL12	21	P52815	3	3	12	0	0	0	*
39S ribosomal protein L22, mitochondrial	MRPL22	24	Q9NWU5	3	2	14	0	0	0	*
39S ribosomal protein L44, mitochondrial	MRPL44	38	Q9H9J2	3	2	9	0	0	0	*
40S ribosomal protein S17	RPS17	16	P08708	3	3	32	0	0	0	*
5'-3' exoribonuclease 1	XRN1	194	Q8IZH2	3	3	2	0	0	0	*
60S ribosomal protein L18a	RPL18A	21	Q02543	3	2	10	0	0	0	*
Aspartyl/asparaginyl beta-hydroxylase	ASPH	86	Q12797	3	3	6	0	0	0	*
BAG family molecular chaperone regulator 2	BAG2	24	O95816	3	2	8	0	0	0	*
Complement component 1 Q subcomponent-binding protein, mitochondrial	C1QBP	31	Q07021	3	3	12	0	0	0	*

Protein Name	Symbol	Molecular Weight (kDa)	Accession Number	Total Spectra: FLAG IP	Unique Peptides: FLAG IP	Percent Coverage: FLAG IP	Total Spectra: Control	Unique Peptides: Control	Percent Coverage: Control	Fold Spectra Increase: IP / Control
CUG-BP- and ETR-3-like factor 1	CUGBP1	52	Q92879	3	3	5	0	0	0	*
ELAV-like protein 2	ELAVL2	40	Q12926	3	2	5	0	0	0	*
Eukaryotic translation initiation factor 3 subunit I	EIF3I (EIF3S2)	37	Q13347	3	2	6	0	0	0	*
Eukaryotic translation initiation factor 4 gamma 3	EIF4G3	177	O43432	3	3	2	0	0	0	*
Guanine nucleotide-binding protein subunit beta-2-like 1	GNB2L1	35	P63244	3	2	9	0	0	0	*
Importin subunit alpha-2	KPNA2	58	P52292	3	3	6	0	0	0	*
Microtubule-associated protein 4	MAP4	121	P27816	3	2	2	0	0	0	*
Myb-binding protein 1A	MYBBP1A	149	Q9BQG0	3	2	1	0	0	0	*
Partner of Y14 and mago	WTBG	23	Q9BRP8	3	2	17	0	0	0	*
Protein FAM98A	FAM98A	55	Q8NCA5	3	2	6	0	0	0	*
Protein LSM12 homolog	LSM12	22	Q3MHD2	3	2	14	0	0	0	*
Protein PAT1 homolog 1	PATL1	87	Q86TB9	3	2	3	0	0	0	*
Replication factor C subunit 4	RFC4	40	P35249	3	3	8	0	0	0	*
RNA-binding protein 39	RBM39	59	Q14498	3	3	6	0	0	0	*
RuvB-like 2	RUVBL2	51	Q9Y230	3	3	7	0	0	0	*
Transcriptional activator protein Pur-beta	PURB	33	Q96QR8	3	2	6	0	0	0	*
Transitional endoplasmic reticulum ATPase	VCP	89	P55072	3	2	3	0	0	0	*
U2-associated protein SR140	SR140	118	O15042	3	3	4	0	0	0	*
U4/U6 small nuclear ribonucleoprotein Prp3	PRPF3	78	O43395	3	3	5	0	0	0	*
UPP0568 protein C14orf166	C14orf166	28	Q9NYF8	3	3	16	0	0	0	*
Zinc finger CCH domain-containing protein 11A	ZC3H11A	89	O75152	3	2	4	0	0	0	*
Zinc finger protein 346	ZNF346	33	Q9UL40	3	2	9	0	0	0	*
116 kDa U5 small nuclear ribonucleoprotein component	EFTUD2	109	Q15029	3	3	3	2	1	1	1.5
28S ribosomal protein S22, mitochondrial	MRPS22	41	P82650	3	2	6	1	1	3	3.0
60S ribosomal protein L15	RPL15	24	P61313	3	2	8	1	1	4	3.0

Protein Name	Symbol	Molecular Weight (kDa)	Accession Number	Total Spectra: FLAG IP	Unique Peptides: FLAG IP	Percent Coverage: FLAG IP	Total Spectra: Control	Unique Peptides: Control	Percent Coverage: Control	Fold Spectra Increase: IP / Control
60S ribosomal protein L32	RPL32	16	B2R4Q3	3	2	15	1	1	7	3.0
Leucine-rich repeat-containing protein 15	LRRCL15	64	Q8TF66	3	3	6	1	1	1	3.0
PERQ amino acid-rich with GYF domain-containing protein 2	GIGYF2	150	Q6Y7W6	3	2	2	1	1	1	3.0
Small nuclear ribonucleoprotein Sm D2	SNRPD2	14	P62316	3	2	16	2	1	8	1.5
Ubiquitin-associated protein 2-like	UBAP2L	115	Q14157	3	2	2	2	1	1	1.5
26S proteasome non-ATPase regulatory subunit 2	PSMD2	100	Q13200	3	3	4	2	2	3	1.5
40S ribosomal protein S13	RPS13	17	P62277	3	2	13	2	2	13	1.5
Phosphoglycerate mutase family member 5	PGAM5	32	Q96HS1	3	3	11	2	2	7	1.5
Vimentin	VIM	54	P08670	3	2	4	2	2	4	1.5
28S ribosomal protein S34, mitochondrial	MIRPS34	26	P82930	2	2	7	0	0	0	*
39S ribosomal protein L48, mitochondrial	MRPL48	24	Q96GC5	2	2	11	0	0	0	*
40S ribosomal protein S24	RPS24	15	P62847	2	2	9	0	0	0	*
5'-3' exoribonuclease 2	XRN2	109	Q9H0D6	2	2	3	0	0	0	*
60S ribosomal protein L13a	RPL13A	24	P40429	2	2	8	0	0	0	*
60S ribosomal protein L21	RPL21	19	Q61AX2	2	2	14	0	0	0	*
ATP synthase subunit alpha, mitochondrial	ATP5A1	60	P25705	2	2	5	0	0	0	*
Calcium-binding mitochondrial carrier protein SCaMC-3	SLC25A23	52	Q9BV35	2	2	5	0	0	0	*
Cell division protein kinase 4	CDK4	34	P11802	2	2	6	0	0	0	*
Cleavage and polyadenylation specificity factor subunit 1	CPSF1	161	Q10570	2	2	2	0	0	0	*
DnaJ homolog subfamily B member 6	DNAJB6	36	O75190	2	2	7	0	0	0	*
Eukaryotic translation initiation factor 2 subunit 3	EIF2S3	51	P41091	2	2	5	0	0	0	*
Eukaryotic translation initiation factor 3 subunit A	EIF3A (EIF3S10)	167	Q14152	2	2	2	0	0	0	*
Eukaryotic translation initiation factor 3 subunit H	EIF3H (EIF3S3)	40	O15372	2	2	5	0	0	0	*
Glutaminyl-peptide cyclotransferase-like protein	QPCTL	43	Q9NXS2	2	2	5	0	0	0	*

Protein Name	Symbol	Molecular Weight (kDa)	Accession Number	Total Spectra: FLAG IP	Unique Peptides: FLAG IP	Percent Coverage: FLAG IP	Total Spectra: Control	Unique Peptides: Control	Percent Coverage: Control	Fold Spectra Increase: IP / Control
Nascent polypeptide-associated complex subunit alpha	NACA	23	Q13765	2	2	13	0	0	0	*
Neuroblast differentiation-associated protein AHNAK	AHNAK	629	Q09666	2	2	0	0	0	0	*
Nucleolar protein 14	NOP14	98	P78316	2	2	3	0	0	0	*
Nucleolar protein 16	NOP16	21	Q9Y3C1	2	2	14	0	0	0	*
Periodic tryptophan protein 2 homolog	PWP2	102	Q15269	2	2	3	0	0	0	*
RING finger protein 10	RNF10	90	Q8N5U6	2	2	3	0	0	0	*
S1 RNA-binding domain-containing protein 1	SRBD1	112	Q8N5C6	2	2	2	0	0	0	*
Superkiller viralicidin activity 2-like 2	SKIV2L2	118	P42285	2	2	2	0	0	0	*
Transcriptional activator protein Pur-alpha	PURA	35	Q00577	2	2	10	0	0	0	*
U4/U6.U5 tri-snRNP-associated protein 1	SART1	90	O43290	2	2	5	0	0	0	*
D-3-phosphoglycerate dehydrogenase	PHGDH	57	O43175	2	2	5	1	1	3	2.0
Elongation factor 1-gamma	EEF1G	50	Q53YD7	2	2	5	1	1	3	2.0
Protein argonaute-2	EIF2C2	97	Q9UKV8	2	2	3	1	1	2	2.0
Protein KIAA1967	KIAA1967	103	Q8N163	2	2	2	1	1	1	2.0
Protein SDA1 homolog	SDAD1	80	Q9NVU7	2	2	3	1	1	1	2.0
Triosephosphate isomerase	TPI1	27	P60174	2	2	10	1	1	5	2.0

Table 2

Nuclear hnRNP cluster

TDP-43 interacting proteins found in the Nuclear/Splicing cluster. The references cited here may be found in the Supplementary References.

Name	Symbol	Function	Supplementary Reference #
ATP-dependent RNA helicase A	DHX9	transcription / translation	1,2
Heterogeneous nuclear ribonucleoprotein U	HNRNPU (HNRPU)	transcription / mRNA stability	3,4
Heterogeneous nuclear ribonucleoproteins C1/C2	HNRNPC (HNRPC)	splicing / mRNA stability	5,6
Heterogeneous nuclear ribonucleoproteins A2/B1	HNRNPA2B1 (HNRPA2B1)	splicing	7
Heterogeneous nuclear ribonucleoprotein U-like protein 1	HNRNPUL1 (HNRPUL1)	mRNA transport	8
Heterogeneous nuclear ribonucleoprotein A1	HNRNPA1 (HNRPA1)	splicing / mRNA stability	5,9
Heterogeneous nuclear ribonucleoprotein M	HNRNPM (HNRPM)	splicing	5
Poly(rC)-binding protein 2	PCBP2	translation	10
Heterogeneous nuclear ribonucleoprotein H	HNRNPH1 (HNRPH1)	splicing	5
Heterogeneous nuclear ribonucleoprotein A3	HNRNPA3 (HNRPA3)	mRNA transport	11
Heterogeneous nuclear ribonucleoprotein G	RBMX	splicing	12
Polyrimidine tract-binding protein 1	PTBPI	splicing	13
Splicing factor, arginine/serine-rich 7	SFRS7	splicing	14
U5 small nuclear ribonucleoprotein 200 kDa helicase	SNRNP200 (ASCC3L1)	splicing	15
Poly(rC)-binding protein 1	PCBP1	transcription / translation / mRNA stability	16
Splicing factor, arginine/serine-rich 6	SFRS6	splicing	17
Nuclear RNA export factor 1	NXF1	mRNA transport	18
Heterogeneous nuclear ribonucleoprotein R	HNRNPR (HNRPR)	splicing / mRNA stability	19
Nuclear cap-binding protein subunit 1	NCBP1	splicing / mRNA transport	20,21
Heterogeneous nuclear ribonucleoprotein A0	HNRNPA0 (HNRPA0)	Unknown	22
U2 small nuclear ribonucleoprotein A'	SNRPA1	splicing	7

Table 3

Cytoplasmic translational cluster

TDP-43 interacting proteins found in the Cytoplasmic/Translation cluster. The references cited here may be found in the Supplementary References.

Name	Symbol	Function	Reference
40S ribosomal protein S11	RPS11	40S ribosome subunit	24
40S ribosomal protein S14	RPS14	40S ribosome subunit	24
40S ribosomal protein S16	RPS16	40S ribosome subunit	24
40S ribosomal protein S18	RPS18	40S ribosome subunit	24
40S ribosomal protein S2	RPS2	40S ribosome subunit	24
40S ribosomal protein S20	RPS20	40S ribosome subunit	24
40S ribosomal protein S23	RPS23	40S ribosome subunit	24
40S ribosomal protein S24	RPS24	40S ribosome subunit	24
40S ribosomal protein S25	RPS25	40S ribosome subunit	24
40S ribosomal protein S3	RPS3	40S ribosome subunit	24
40S ribosomal protein S3a	RPS3A	40S ribosome subunit	24
40S ribosomal protein S4, X isoform	RPS4X	40S ribosome subunit	24
40S ribosomal protein S6	RPS6	40S ribosome subunit	24
40S ribosomal protein S7	RPS7	40S ribosome subunit	24
40S ribosomal protein S9	RPS9	40S ribosome subunit	24
40S ribosomal protein SA	RPSA	40S ribosome subunit	24
60S acidic ribosomal protein P0	RPLP0	60S ribosome subunit	24
60S ribosomal protein L10a	RPL10A	60S ribosome subunit	24
60S ribosomal protein L11	RPL11	60S ribosome subunit	24
60S ribosomal protein L12	RPL12	60S ribosome subunit	24
60S ribosomal protein L13	RPL13	60S ribosome subunit	24
60S ribosomal protein L13a	RPL13A	60S ribosome subunit	24
60S ribosomal protein L14	RPL14	60S ribosome subunit	24

Name	Symbol	Function	Reference
60S ribosomal protein L17	RPL17	60S ribosome subunit	24
60S ribosomal protein L18A	RPL18A	60S ribosome subunit	24
60S ribosomal protein L19	RPL19	60S ribosome subunit	24
60S ribosomal protein L21	RPL21	60S ribosome subunit	24
60S ribosomal protein L22	RPL22	60S ribosome subunit	24
60S ribosomal protein L23	RPL23	60S ribosome subunit	24
60S ribosomal protein L23a	RPL23A	60S ribosome subunit	24
60S ribosomal protein L26	RPL26	60S ribosome subunit	24
60S ribosomal protein L28	RPL28	60S ribosome subunit	24
60S ribosomal protein L3	RPL3	60S ribosome subunit	24
60S ribosomal protein L31	RPL31	60S ribosome subunit	24
60S ribosomal protein L32	RPL32	60S ribosome subunit	24
60S ribosomal protein L35	RPL35	60S ribosome subunit	24
60S ribosomal protein L4	RPL4	60S ribosome subunit	24
60S ribosomal protein L5	RPL5	60S ribosome subunit	24
60S ribosomal protein L6	RPL6	60S ribosome subunit	24
60S ribosomal protein L7	RPL7	60S ribosome subunit	24
60S ribosomal protein L7a	RPL7A	60S ribosome subunit	24
60S ribosomal protein L8	RPL8	60S ribosome subunit	24
Eukaryotic translation initiation factor 4 gamma 1	EIF4G1	translation initiation factor	25
Elongation factor 2	EEF2 (EF2)	translation elongation factor	26
Eukaryotic translation initiation factor 3 subunit I	EIF3I (EIF3S2)	translation initiation factor	27
Eukaryotic translation initiation factor 3 subunit A	EIF3A (EIF3S10)	translation initiation factor	27
Eukaryotic translation initiation factor 3 subunit B	EIF3B (PRT1)	translation initiation factor	27
Eukaryotic translation initiation factor 3 subunit C	EIF3C (EIF3S8)	translation initiation factor	27
Eukaryotic translation initiation factor 3 subunit H	EIF3H (EIF3S3)	translation initiation factor	27

Table 4

TDP-43 associated stress granule proteins

Stress granule proteins found to co-immunoprecipitate with TDP-43.

Name	Symbol
Protein argonaute-2	EIF2C2
Caprin-1	CAPRIN1
Eukaryotic translation initiation factor 3 (5 subunits)	EIF3
Eukaryotic translation initiation factor 4 gamma (2 subunits)	EIF4G
Far upstream element-binding protein 2	KHSRP
Ras GTPase-activating protein-binding protein 1	G3BP1
ELAV-like protein 1	ELAVL1
Polyadenylate-binding protein 1	PABPC1
Probable ATP-dependent RNA helicase DDX6	DDX6
Plakophilin-1	PKP1
Double-stranded RNA-binding protein Staufien homolog 1	STAU1
Ubiquitin carboxyl-terminal hydrolase 10	USP10
Eukaryotic initiation factor 4A (2 subunits)	EIF4A
Nuclease sensitive element-binding protein 1	YBX1
40S Ribosome (20 subunits)	40S